

Approximation properties relative to continuous scale space for hybrid discretizations of Gaussian derivative operators

Tony Lindeberg

Received: date / Accepted: date

Abstract This paper presents an analysis of properties of two hybrid discretization methods for Gaussian derivatives, based on convolutions with either the normalized sampled Gaussian kernel or the integrated Gaussian kernel followed by central differences. The motivation for studying these discretization methods is that in situations when multiple spatial derivatives of different order are needed at the same scale level, they can be computed significantly more efficiently compared to more direct derivative approximations based on explicit convolutions with either sampled Gaussian kernels or integrated Gaussian kernels.

While these computational benefits do also hold for the genuinely discrete approach for computing discrete analogues of Gaussian derivatives, based on convolution with the discrete analogue of the Gaussian kernel followed by central differences, the underlying mathematical primitives for the discrete analogue of the Gaussian kernel, in terms of modified Bessel functions of integer order, may not be available in certain frameworks for image processing, such as when performing deep learning based on scale-parameterized filters in terms of Gaussian derivatives, with learning of the scale levels. The hybrid discretizations studied in this paper do, from this perspective, offer a computationally more efficient way of implementing deep networks based on Gaussian derivatives for such use cases.

In this paper, we present a characterization of the properties of these hybrid discretization methods, in terms of quantitative performance measures concerning the amount of spatial smoothing that they imply, as well as the relative

consistency of scale estimates obtained from scale-invariant feature detectors with automatic scale selection, with an emphasis on the behaviour for very small values of the scale parameter, which may differ significantly from corresponding results obtained from the fully continuous scale-space theory, as well as between different types of discretization methods.

The presented results are intended as a guide, when designing as well as interpreting the experimental results of scale-space algorithms that operate at very fine scale levels.

Keywords Scale · Discrete · Continuous · Gaussian kernel · Gaussian derivative · Scale space

1 Introduction

When to implement the Gaussian derivative operators in scale-space theory, the composed effect of the underlying Gaussian smoothing operation and the following derivative computations need to be discretized in some way. Since a majority of the formulations of scale-space theory are expressed for continuous signals or continuous images, it is essential to also ensure that the desirable properties of the theoretically well-founded scale-space representations are to a sufficiently good degree of approximation transferred to the discrete implementation. Simultaneously, the amount of necessary computations needed for the implementation may often constitute a limiting factor when to choose an appropriate discretization method for expressing actual algorithms are to operate on the discrete data to be analyzed.

While one may argue that at sufficiently coarse scale levels, it ought to be the case that the choice of discretization method should not significantly affect the quality of the output of a scale-space algorithm, at very fine scale levels, on the other hand, the properties of a discretized implementa-

The support from the Swedish Research Council (contracts 2022-02969) is gratefully acknowledged.

Tony Lindeberg
Computational Brain Science Lab, Division of Computational Science and Technology, KTH Royal Institute of Technology, SE-100 44 Stockholm, Sweden. E-mail: tony@kth.se

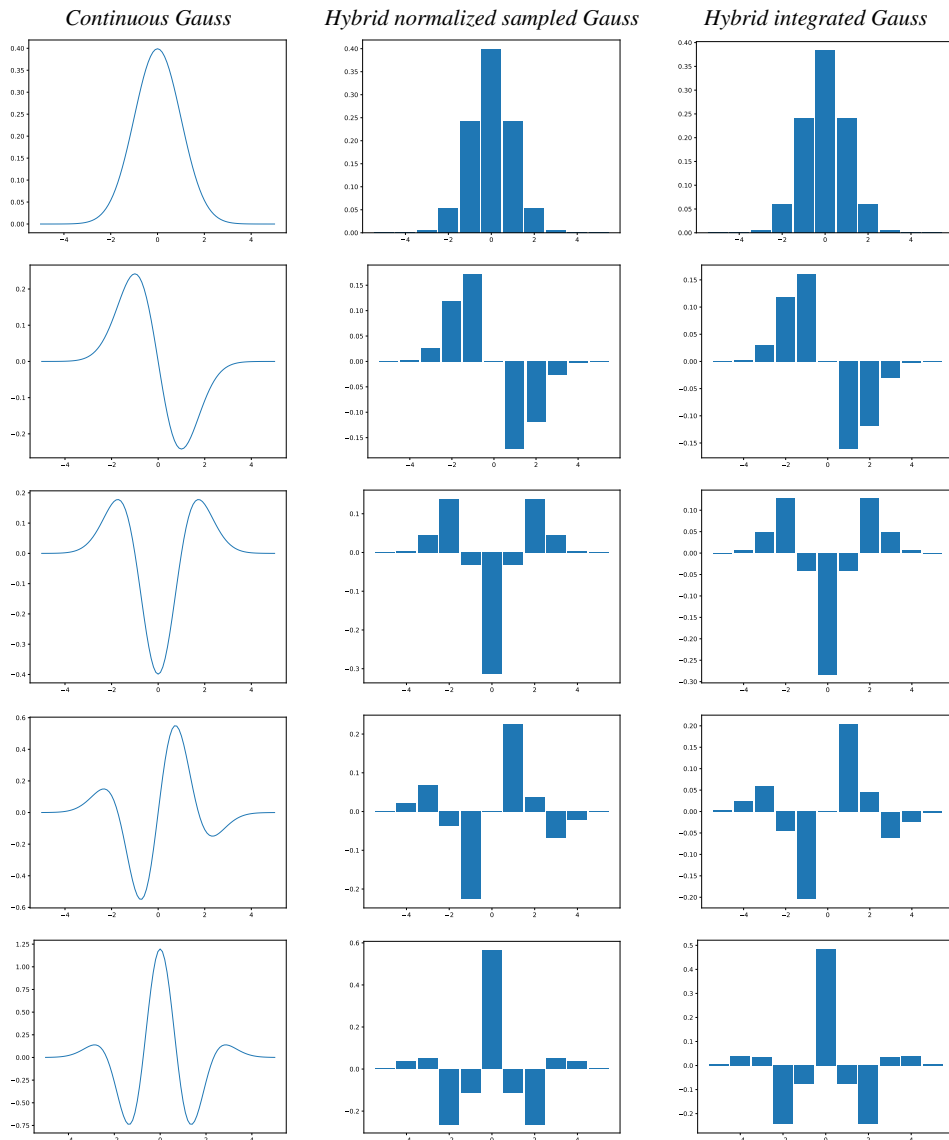


Fig. 1: Graphs of the main types of Gaussian smoothing kernels as well as of the equivalent convolution kernels for the hybrid discretizations of Gaussian derivative operators considered specially in this paper, here at the scale $\sigma = 1$, with the raw smoothing kernels in the top row and the order of spatial differentiation increasing downwards up to order 4: (left column) continuous Gaussian kernel and continuous Gaussian derivatives, (middle column) normalized sampled Gaussian kernel and central differences applied to the normalized sampled Gaussian kernel, (right column) integrated Gaussian kernel and central differences applied to the integrated Gaussian kernel. Note that the scaling of the vertical axis may vary between the different subfigures. (Horizontal axis: the 1-D spatial coordinate $x \in [-5, 5]$.) (Graphs of the regular sampled Gaussian derivative kernels, the regular integrated Gaussian derivative kernels and the discrete analogues of Gaussian derivatives up to order 4 are shown in Figure 1 in (Lindeberg 2024).)

tion of notions from scale-space theory may depend strongly on the actual choice of a discretization method.

The subject of this article, is to perform a more detailed analysis of a class of hybrid discretization methods, based on convolution with either the sampled Gaussian kernel, the normalized sampled Gaussian kernel or the integrated Gaussian kernel, followed by computations of discrete derivative approximations by central difference operators, and specifically characterize the degree of approximation of continuous

expressions in scale-space theory that these discretization give rise to, see Figure 1 for examples of graphs of equivalent convolution kernels corresponding to these discretization methods. This class of discretization methods was outlined among extensions to future work in Section 6.1 in (Lindeberg 2024), and was also complemented with a description about theoretical scale-space properties of these discretizations in Footnote 13 in (Lindeberg 2024). There were, however, not further in-depth characterizations of the

approximation properties of these discretizations with regard to what results they lead to in relation to corresponding results from the continuous scale-space theory.

The main goal of this paper is to address topic in terms of a set of quantitative performance measures, intended to be of general applicability for different types of visual tasks. Specifically, we will perform comparisons to the other main types of discretization methods considered in (Lindeberg 2024), based on either (i) explicit convolutions with sampled Gaussian derivative kernels, (ii) explicit convolutions with integrated Gaussian derivative kernels, or (iii) convolution with the discrete analogue of the Gaussian kernel followed by computations of discrete derivative approximations by central difference operators.

A main rationale for studying this class of hybrid discretizations is that in situations when multiple Gaussian derivative responses of different orders are needed at the same scale level, these hybrid discretizations imply substantially lower amounts of computations, compared to explicit convolutions with either sampled Gaussian derivative kernels or integrated Gaussian derivative kernels for each order of differentiation. The reason for this better computational efficiency, which also holds for the discretization approach based on convolution with the discrete analogue of the Gaussian kernel followed by central differences, is that the spatial smoothing part of the operation, which is performed over a substantially larger number of input data than the small-support central difference operators, can be shared between the different orders of differentiation.

A further rationale for studying these hybrid discretizations is that in certain applications, such as the use of Gaussian derivative operators in deep learning architectures (Jacobsen *et al.* 2016, Lindeberg 2021, 2022, Pinteá *et al.* 2021, Sangalli *et al.* 2022, Penaud-Polge *et al.* 2022, Gavilima-Pilataxi and Ibarra-Fiallo 2023), the modified Bessel functions of integer order, as used as the underlying mathematical primitives in the discrete analogue of the Gaussian kernel, may, however, not be fully available in the framework used for implementing the image processing operations. For this reason, the hybrid discretizations may, for efficiency reasons, constitute an interesting alternative to using discretizations in terms of either sampled Gaussian derivative kernels or integrated Gaussian derivative kernels, when to implement certain tasks, such as learning of the scale levels by backpropagation, which usually require full availability of the underlying mathematical primitives the scale-parameterized filter family with regard to the deep learning framework, to be able to propagate the gradients between the layers in the deep learning architecture.

Deliberately, the scope of this paper will therefore be rather narrow, and mainly to serve as a complement to the in-depth treatment of discretizations of the Gaussian smoothing operation and the Gaussian derivative operators, and as

a specific complement to the outline of the hybrid discretizations in the future work section in (Lindeberg 2024).

We will therefore not consider other theoretically well-founded discretizations of scale-space operations (Wang 1999, Lim and Stiehl 2003, Tschirsch and Kuijper 2015, Slavik and Stehlík 2015, Rey-Otero and Delbracio 2016). Nor will we consider alternative approaches in terms of pyramid representations (Burt and Adelson 1983, Crowley 1984, Simoncelli *et al.* 1992, Simoncelli and Freeman 1995, Lindeberg and Bretzner 2003, Crowley and Riff 2003, Lowe 2004), Fourier-based implementations, splines (Unser *et al.* 1991, 1993, Wang and Lee 1998, Bouma *et al.* 2007, Bekkers 2020, Zheng *et al.* 2022) or recursive filters (Deriche 1992, Young and van Vliet 1995, van Vliet *et al.* 1998, Geusebroek *et al.* 2003, Farnéback and Westin 2006, Charalampidis 2016).

Instead, we will focus on a narrow selection of five specific methods, for implementing Gaussian derivative operations in terms of purely discrete convolution operations, and then with the emphasis on the behaviour for very small values of the scale parameter.

2 Discretization methods for Gaussian derivative operators

Given the definition of a scale-space representation of a one-dimensional continuous signal (Iijima 1962; Witkin 1983; Koenderink 1984; Koenderink and van Doorn 1987, 1992; Lindeberg 1993a, 1994, 2011; Florack 1997; Sporring *et al.* 1997; Weickert *et al.* 1999; ter Haar Romeny 2003), the 1-D Gaussian kernel is defined according to

$$g(x; s) = \frac{1}{\sqrt{2\pi s}} e^{-x^2/2s}, \quad (1)$$

where the parameter s is referred to as the scale parameter, and any 1-D Gaussian derivative kernel for spatial differentiation order α is defined according to

$$g_{x^\alpha}(x; s) = \partial_{x^\alpha} g(x; s), \quad (2)$$

with the associated computation of Gaussian derivative responses from any 1-D input signal $f(x)$, in turn, defined according to

$$L_{x^\alpha}(x; s) = \int_{\xi \in \mathbb{R}} g_{x^\alpha}(\xi; s) f(x - \xi) d\xi. \quad (3)$$

Let us first consider the following ways of approximating the Gaussian convolution operation for discrete data, based on convolutions with either:

- the sampled Gaussian kernel defined according to

$$T_{\text{sampl}}(n; s) = g(n; s), \quad (4)$$

- the normalized sampled Gaussian kernel defined according to

$$T_{\text{normsAMPL}}(n; s) = \frac{g(n; s)}{\sum_{m \in \mathbb{Z}} g(m; s)}, \quad (5)$$

- the integrated Gaussian kernel defined according to (Lindeberg 1993a Equation (3.89))

$$T_{\text{int}}(n; s) = \int_{x=n-1/2}^{n+1/2} g(x; s) dx, \quad (6)$$

- or the discrete analogue of the Gaussian kernel defined according to (Lindeberg 1990 Equation (19))

$$T_{\text{disc}}(n; s) = e^{-s} I_n(s), \quad (7)$$

where $I_n(s)$ denotes the modified Bessel functions of integer order.

Then, we consider the following previously studied methods for discretizing the computation of Gaussian derivative operators, in terms of either:

- convolutions with sampled Gaussian derivative kernels according to

$$T_{\text{sAMPL},x^\alpha}(n; s) = g_{x^\alpha}(n; s), \quad (8)$$

- convolutions with integrated Gaussian derivative kernels according to (Lindeberg 2024 Equation (54))

$$T_{\text{int},x^\alpha}(n; s) = \int_{x=n-1/2}^{n+1/2} g_{x^\alpha}(x; s) dx, \quad (9)$$

- the genuinely discrete approach corresponding to convolution with the discrete analogue of the Gaussian kernel $T_{\text{disc}}(n; s)$ according to (7) followed by central difference operators, thus corresponding to the equivalent discrete approximation kernel (Lindeberg 1993b Equation (58))

$$T_{\text{disc},x^\alpha}(n; s) = (\delta_{x^\alpha} T_{\text{disc}})(n; s). \quad (10)$$

Here, the central difference operators are for orders 1 and 2 defined according to

$$\delta_x = (-\frac{1}{2}, 0, +\frac{1}{2}), \quad (11)$$

$$\delta_{xx} = (+1, -2, +1), \quad (12)$$

and of the following forms for higher values of α :

$$\delta_{x^\alpha} = \begin{cases} \delta_x (\delta_{xx})^i & \text{if } \alpha = 1 + 2i, \\ (\delta_{xx})^i & \text{if } \alpha = 2i, \end{cases} \quad (13)$$

for integer i , where the special cases $\alpha = 3$ and $\alpha = 4$ then correspond to the difference operators

$$\delta_{xxx} = (-\frac{1}{2}, +1, 0, -1, +\frac{1}{2}), \quad (14)$$

$$\delta_{xxxx} = (+1, -4, +6, -4, +1). \quad (15)$$

In addition to the above, already studied discretization methods in (Lindeberg 2024), we will here specifically consider the properties of the following hybrid methods, in terms of either:

- the hybrid approach corresponding to convolution with the normalized sampled Gaussian kernel $T_{\text{normsAMPL}}(n; s)$ according to (5) followed by central difference operators, thus corresponding to the equivalent discrete approximation kernel (Lindeberg 2024 Equation (116))

$$T_{\text{hybr-sAMPL},x^\alpha}(n; s) = (\delta_{x^\alpha} T_{\text{normsAMPL}})(n; s), \quad (16)$$

- the hybrid approach corresponding to convolution with the integrated Gaussian kernel $T_{\text{int}}(n; s)$ according to (6) followed by central difference operators, thus corresponding to the equivalent discrete approximation kernel (Lindeberg 2024 Equation (117))

$$T_{\text{hybr-int},x^\alpha}(n; s) = (\delta_{x^\alpha} T_{\text{int}})(n; s). \quad (17)$$

A motivation for introducing the latter hybrid discretization methods (16) and (17), based on convolutions with the normalized sampled Gaussian kernel (5) or the integrated Gaussian kernel (6) followed by central difference operators of the form (13), is that these discretization methods have substantially better computational efficiency, compared to explicit convolutions with either the sampled Gaussian derivative kernels (8) or the integrated Gaussian derivative kernels (9), in situations when spatial derivatives of multiple orders are needed at the same scale level.

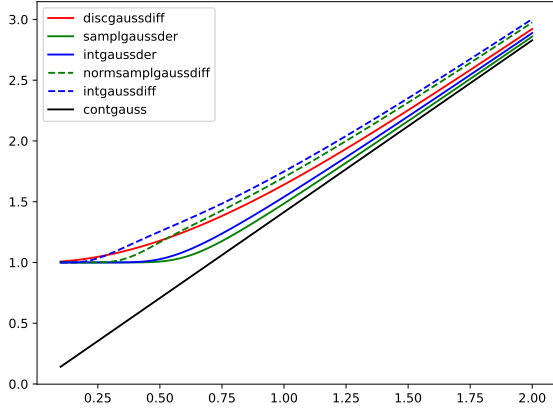
The reason for this is that the same spatial smoothing stage can then be shared between the computations of discrete derivative approximations for the different orders of spatial differentiation, thus implying that these hybrid methods will be as computationally efficient as the genuinely discrete approach, based on convolution with the discrete analogue of the Gaussian kernel (7) followed by central differences of the form (13), and corresponding to equivalent convolution kernels of the form (10).

3 Characterization of the effective amount of spatial smoothing in discrete approximations of Gaussian derivatives in terms of spatial spread measures

To measure how well these different discretization of the Gaussian derivative operators reflect properties of the underlying continuous Gaussian derivatives, let us first consider quantifications in terms of the following spatial spread measure, defined from the absolute value of each equivalent discrete derivative approximation kernel (Lindeberg 2024 Equation (80)):

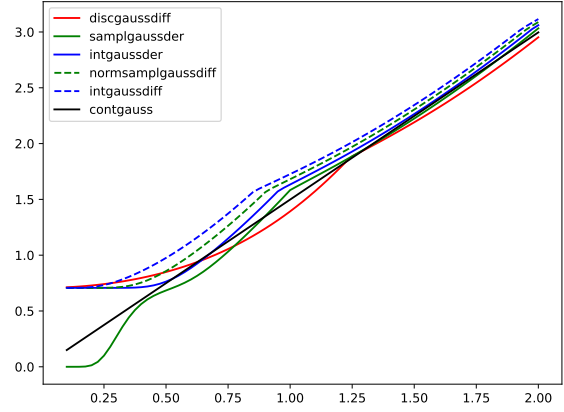
$$\sqrt{V(|T_{x^\alpha}(\cdot; s)|)} \quad (18)$$

Spatial spread measures for 1st-order derivative kernels



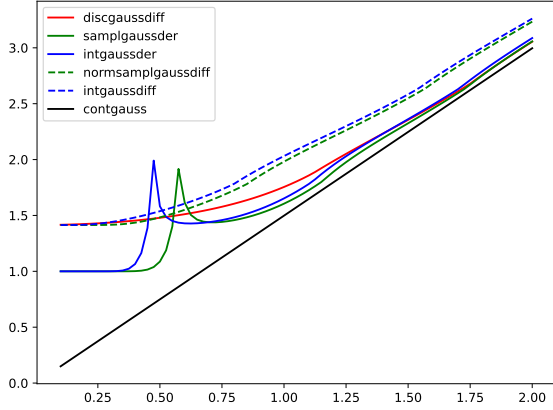
(a) Case: $\alpha = 1$. Note that the spatial spread measures for the spatial smoothing kernels combined with central differences are delimited from below by the spatial variance of the absolute value of the first-order central difference operator $|\delta_x|$, which is $\sqrt{V(|\delta_x|)} = 1$.

Spatial spread measures for 2nd-order derivative kernels



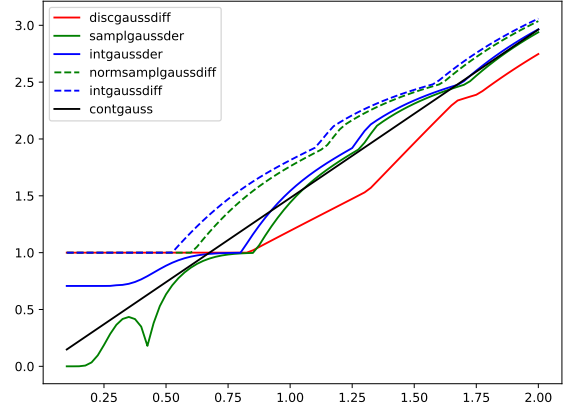
(b) Case: $\alpha = 2$. Note that the spatial spread measures for the spatial smoothing kernels combined with central differences are delimited from below by the spatial variance of the absolute value of the second-order central difference operator $|\delta_{xx}|$, which is $\sqrt{V(|\delta_{xx}|)} = 1/\sqrt{2}$.

Spatial spread measures for 3rd-order derivative kernels



(c) Case: $\alpha = 3$. Note that the spatial spread measures for the spatial smoothing kernels combined with central differences are delimited from below by the spatial variance of the absolute value of the third-order central difference operator $|\delta_{xxx}|$, which is $\sqrt{V(|\delta_{xxx}|)} = \sqrt{2}$.

Spatial spread measures for 4th-order derivative kernels



(d) Case: $\alpha = 4$. Note that the spatial spread measures for the spatial smoothing kernels combined with central differences are delimited from below by the spatial variance of the absolute value of the fourth-order central difference operator $|\delta_{xxxx}|$, which is $\sqrt{V(|\delta_{xxxx}|)} = 1$.

Fig. 2: Graphs of the *spatial spread measure* $\sqrt{V(|T_{x^\alpha}(\cdot; s)|)}$ according to (18) for different discrete approximations of Gaussian derivative kernels of order α : (i) for either discrete analogues of Gaussian derivative kernels $T_{\text{disc},x^\alpha}(n; s)$ according to (10), corresponding to convolutions with the discrete analogue of the Gaussian kernel $T_{\text{disc}}(n; s)$ according to (7) followed by central differences according to (13), (ii) sampled Gaussian derivative kernels $T_{\text{sampl},x^\alpha}(n; s)$ according to (8), (iii) integrated Gaussian derivative kernels $T_{\text{int},x^\alpha}(n; s)$ according to (9), (iv) the hybrid discretization kernel $T_{\text{hybr-sampl},x^\alpha}(n; s)$ according to (16), corresponding to convolution with the normalized sampled Gaussian kernel $T_{\text{normsampl}}(n; s)$ according to (5) followed by central differences according to (13), and (v) the hybrid discretization kernel $T_{\text{hybr-int},x^\alpha}(n; s)$ according to (17), corresponding to convolution with the integrated Gaussian kernel $T_{\text{int}}(n; s)$ according to (6) followed by central differences according to (13). (Horizontal axis: Scale parameter in units of $\sigma = \sqrt{s} \in [0.1, 2]$.)

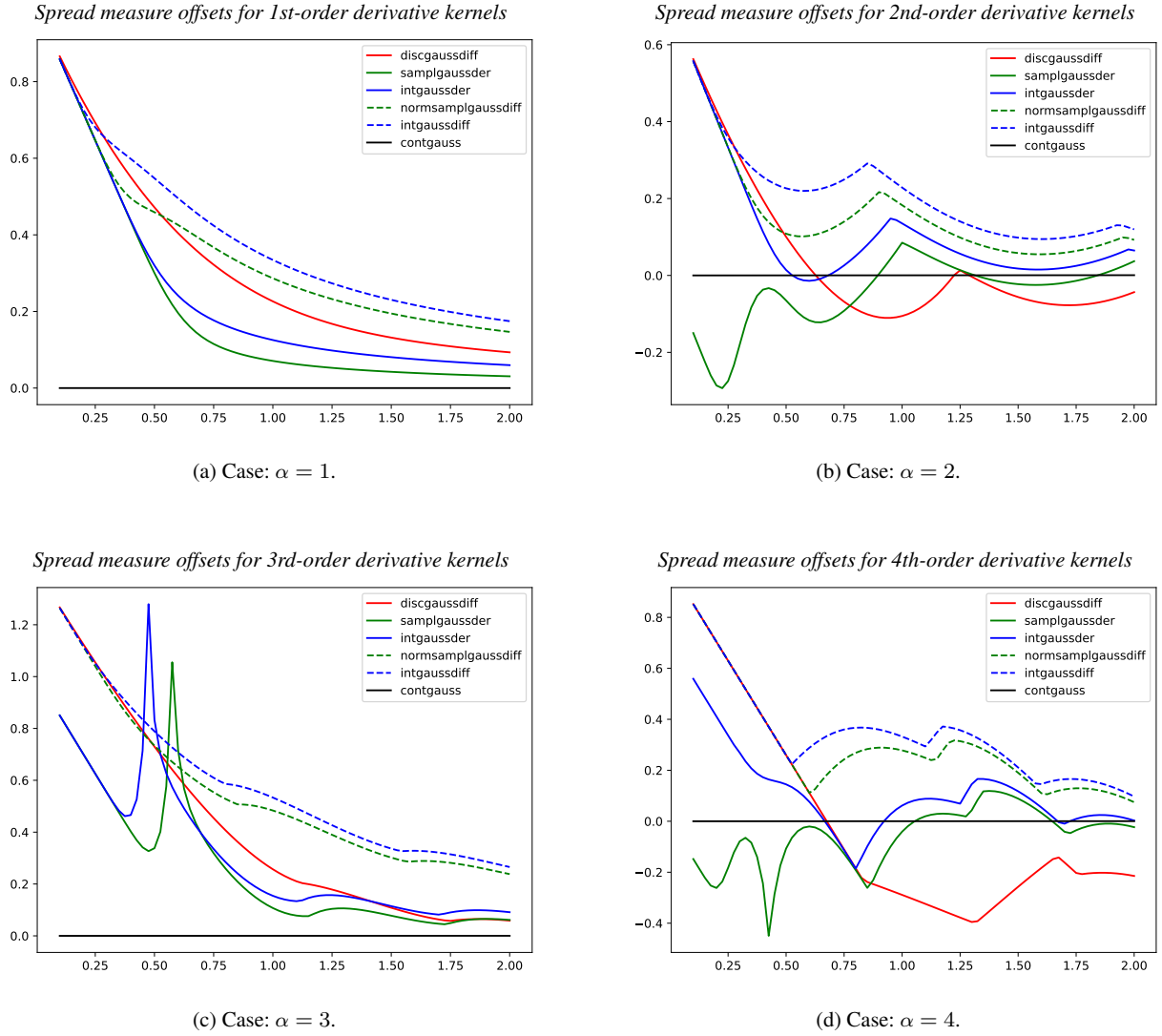


Fig. 3: Graphs of the *spatial spread measure offset* $O_\alpha(s)$, relative to the spatial spread of a continuous Gaussian kernel, according to (19), for different discrete approximations of Gaussian derivative kernels of order α : (i) for either discrete analogues of Gaussian derivative kernels $T_{\text{disc},x^\alpha}(n; s)$ according to (10), corresponding to convolutions with the discrete analogue of the Gaussian kernel $T_{\text{disc}}(n; s)$ according to (7) followed by central differences according to (13), (ii) sampled Gaussian derivative kernels $T_{\text{sampl},x^\alpha}(n; s)$ according to (8), (iii) integrated Gaussian derivative kernels $T_{\text{int},x^\alpha}(n; s)$ according to (9), (iv) the hybrid discretization kernel $T_{\text{hybr-sampl},x^\alpha}(n; s)$ according to (16), corresponding to convolution with the normalized sampled Gaussian kernel $T_{\text{normsampl}}(n; s)$ according to (5) followed by central differences according to (13), and (v) the hybrid discretization kernel $T_{\text{hybr-int},x^\alpha}(n; s)$ according to (17), corresponding to convolution with the integrated Gaussian kernel $T_{\text{int}}(n; s)$ according to (6) followed by central differences according to (13). (Horizontal axis: Scale parameter in units of $\sigma = \sqrt{s} \in [0.1, 2]$.)

To furthermore more explicitly quantify the deviation from the corresponding fully continuous spatial spread measures $\sqrt{V(|g_{x^\alpha}(\cdot; s)|)}$, we also consider the following measures of the offsets of the spatial spread measures (Lindeberg 2024 Equation (81)):

$$O_\alpha(s) = \sqrt{V(|T_{x^\alpha}(\cdot; s)|)} - \sqrt{V(|g_{x^\alpha}(\cdot; s)|)}. \quad (19)$$

Figures 2–3 show the graphs of computing these spatial spread measures over an interval of finer scale values $\sigma = \sqrt{s} \in [0.1, 2]$ for each one of the different discretization methods. As can be seen from these graphs:

- The agreement with the underlying fully continuous spread measures for the continuous Gaussian derivative kernels is substantially better for the genuinely sampled or integrated Gaussian derivative kernels than for the hybrid discretizations based on combining either the normalized sampled Gaussian kernel or the integrated Gaussian kernel with central difference operators.

The hybrid discretization kernels, corresponding to convolutions with either the normalized sampled Gaussian kernel or the integrated Gaussian kernel followed by central differences, generally have substantially larger off-

sets from the underlying continuous theory, than the more direct discretizations in terms of either sampled Gaussian derivative kernels or integrated Gaussian kernels.

In situations when multiple derivatives of different orders α are to be computed at the same scale levels, the hybrid discretization methods are, however, as previously mentioned, computationally much more efficient, implying that the introduction of the hybrid discretizations implies a trade-off between the accuracy in terms of the overall amount of spatial smoothing of the equivalent discrete filters and the computational efficiency of the implementation.

- The agreement with the underlying fully continuous spread measures for the continuous Gaussian derivative kernels is substantially better for the genuinely discrete analogue of Gaussian derivative operators, obtained by first convolving the input data with the discrete analogue of the Gaussian kernel and then applying central difference operators to the spatially smoothing input data, compared to using any of the hybrid discretizations, corresponding to first smoothing the input data with either the normalized sampled Gaussian kernel or the integrated Gaussian kernel, and then applying central difference operators to the spatially smoothed input data.

If, for efficiency reasons, a discretization method is to be chosen, based on combining a first stage of spatial smoothing with a following application of central difference operators, the approach based on using spatial smoothing with the discrete analogue of the Gaussian kernel, in most of the cases, leads to better agreement with the underlying continuous theory, compared to using either the normalized sampled Gaussian kernel or the integrated Gaussian kernel in the first stage of spatial smoothing.

As previously stated, the hybrid discretization methods may, however, anyway be warranted in situations where the underlying modified Bessel functions $I_n(s)$ are not fully available the computational environment where the discrete filtering operations are to be implemented, such as when performing learning of the scale levels in deep networks based on Gaussian derivative operators coupled in cascade.

A further general implication of these results is that, depending on what discretization method is chosen for discretizing the computation of Gaussian derivative responses at fine scales, different values of the spatial scale parameter s will be needed, to obtain a comparable amount of spatial smoothing of the input data for the different discretization methods.

4 Characterization of resulting consistency properties over scale in terms of the accuracy of the scale estimates obtained from integrations with scale selection algorithms

To perform a further evaluation of the hybrid discretization method to consistently process input data over multiple scales, we will characterize the abilities of these methods in a context of automatic scale selection, where hypotheses about local appropriate scale levels are determined from local extrema over scale of scale-normalized derivatives.

For this purpose, we follow a similar methodology as used in (Lindeberg 2024 Section 4). Thus, with now the theory from Section 2 now applied to 2-D image data, by separable application of the 1-D theory along each image dimension, we consider scale-normalized derivative operators defined according to (Lindeberg 1998a, 1998b)

$$\partial_\xi = s^{\gamma/2} \partial_x, \quad \partial_\eta = s^{\gamma/2} \partial_y, \quad (20)$$

with $\gamma > 0$ being a scale normalization power, that is chosen specially adapted for each feature detection task.

4.1 Scale-invariant feature detectors with automatic scale selection

Specifically, we will evaluate the performance of the following types of scale-invariant feature detectors:

- interest detection from scale-space extrema of the scale-normalized Laplacian operator (Lindeberg 1998a Equation (30))

$$\nabla_{norm}^2 L = s (L_{xx} + L_{yy}), \quad (21)$$

or the scale-normalized determinant of the Hessian operator (Lindeberg 1998a Equation (31))

$$\det \mathcal{H}_{norm} L = s^2 (L_{xx} L_{yy} - L_{xy}^2), \quad (22)$$

where we here choose the scale normalization parameter $\gamma = 1$, such that the selected scale level for a Gaussian blob of size s_0

$$f_{\text{blob}, s_0}(x, y) = g_{2D}(x, y; s_0), \quad (23)$$

will for both Laplacian and determinant of the Hessian interest point detection be equal to the size of the blob (Lindeberg 1998a, Equations (36) and (37))

$$\begin{aligned} (\hat{x}, \hat{y}, \hat{s}) &= \operatorname{argmin}_{(x, y; s)} (\nabla^2 L_{\text{blob}, s_0})(x, y; s) \\ &= (0, 0, s_0), \end{aligned} \quad (24)$$

$$\begin{aligned} (\hat{x}, \hat{y}, \hat{s}) &= \operatorname{argmax}_{(x, y; s)} (\det \mathcal{H} L_{\text{blob}, s_0})(x, y; s) \\ &= (0, 0, s_0). \end{aligned} \quad (25)$$

- edge detection from combined

- (i) maxima of the gradient magnitude in the spatial gradient direction e_v reformulated such that the second-order directional derivative L_{vv} in the gradient direction is zero and the third-order directional derivative in the gradient direction L_{vvv} is negative (Lindeberg 1998b Equation (8)) and
- (ii) maxima over scale of the scale-normalized gradient magnitude according to (Lindeberg 1998b Equation (15))

$$L_{v,\text{norm}} = s^{\gamma/2} \sqrt{L_x^2 + L_y^2}, \quad (26)$$

where we here set the scale normalization parameter to (Lindeberg 1998b, Equation (23))

$$\gamma_{\text{edge}} = \frac{1}{2}, \quad (27)$$

such that the selected scale level for an idealized model of a diffuse edge (Lindeberg 1998b Equation (18))

$$f_{\text{edge},s_0}(x, y) = \int_{u=-\infty}^x g(u; s_0) du \quad (28)$$

will be equal to the amount of diffuseness of that diffuse edge

$$\hat{s} = \operatorname{argmax}_s L_{v,\text{norm}}(0, 0; s) = s_0, \quad (29)$$

- ridge detection from combined
 - (i) zero-crossings of the first-order directional derivative in the first principal curvature direction e_p of the Hessian matrix, such that $L_p = 0$ (Lindeberg 1998b Equations (42)), and
 - (ii) minima over scale of the scale-normalized ridge strength in terms the scale-normalized second-order derivative $L_{pp,\text{norm}}$ in the direction e_p according to (Lindeberg 1998b Equation (47)):

$$\begin{aligned} L_{pp,\text{norm}} &= s^\gamma L_{pp} = \\ &= s^\gamma \left(L_{xx} + L_{yy} - \sqrt{(L_{xx} - L_{yy})^2 + 4L_{xy}^2} \right), \end{aligned} \quad (30)$$

where we here choose the scale normalization parameter as (Lindeberg 1998b, Equation (56))

$$\gamma_{\text{ridge}} = \frac{3}{4}, \quad (31)$$

such that the selected scale level for a Gaussian ridge model of the form

$$f_{\text{ridge},s_0}(x, y) = g(x; s_0) \quad (32)$$

will be equal to the width of that idealized ridge model

$$\hat{s} = \operatorname{argmax}_s L_{pp,\text{norm}}(0, 0; s) = s_0, \quad (33)$$

A common property of all these scale-invariant feature detectors is thus the selected scale levels \hat{s} obtained from local extrema over scale will reflect a characteristic scale s_0 in the input data. By evaluating discretization methods of Gaussian derivatives with respect to such scale selection properties, we therefore have a way of formulating a well-defined proxy task for evaluating how well the different types of discretization methods lead to appropriate consistency properties over scales for the numerical implementation of Gaussian derivative operators.

4.2 Experimental methodology

To quantify the performance of the different discretization methods, we will

- compute the selected scale levels $\hat{\sigma} = \sqrt{\hat{s}}$ for different values of the characteristic scale s_0 in the image data, measured in dimension length $\sigma_0 = \sqrt{s_0}$ and
- quantify the deviations from the reference in terms of the relative error measure (Lindeberg 2024 Equation (107))

$$E_{\text{scaleest,rel}}(s) = \sqrt{\frac{\hat{s}}{\hat{s}_{\text{ref}}}} - 1, \quad (34)$$

under variations of the characteristic scale $s = \sigma^2$ in the input image, where the deviations between the selected scale levels $\hat{\sigma}$ and the reference value σ_0 are to be interpreted as results of discretization errors.

When generating input data for different values of the reference scale σ_0 , we will

- for the purpose of Laplacian or determinant of the Hessian interest point detection, use a discrete approximation of Gaussian blob (23) obtained by convolving a 2-D discrete delta function $\delta(x, y)$ with a discrete approximation of a Gaussian kernel along each dimension,
- for the purpose of edge detection, use a discrete approximation of a diffuse edge (28), obtained by convolving a heaviside function $H(x)$ with a discrete approximation of a Gaussian kernel along the x -direction,
- for the purpose of ridge detection, use a discrete approximation of a Gaussian ridge (32), obtained by convolving the 2-D extension of a 1-D discrete delta function $\delta(x)$ along the y -direction with a discrete approximation of a Gaussian kernel along the x -direction.

Since a main purpose of this experiment is to measure the consistency between the characteristic scales in the input with the characteristic scale values obtained by multi-scale processing of the input data, we will

- when evaluating the discretization based on the discrete analogue of Gaussian derivatives, use the discrete analogue of the Gaussian kernel as the discrete convolution kernel when generating the input data,

- when evaluating the discretization method based on sampled Gaussian derivatives, use the sampled Gaussian kernel as the discrete convolution kernel when generating the input data,
- when evaluating the discretization method based on integrated Gaussian derivatives, use the integrated Gaussian kernel as the discrete convolution kernel when generating the input data,
- when evaluating the hybrid method based on convolution with the normalized sampled Gaussian kernel followed by central differences, use the normalized sampled Gaussian kernel as the discrete convolution kernel when generating the input data, and
- when evaluating the hybrid method based on convolution with the integrated Gaussian kernel followed by central differences, use the normalized integrated Gaussian kernel as the discrete convolution kernel when generating the input data.

Thus, the intention is to use an as similar discretization method for generating the input data as will be used when analyzing the same data. Since the generation of the input data will hence differ between the different discretization methods for Gaussian derivatives, some care does therefore need to be taken when to interpret the experimental results.¹

4.3 Experimental results

For generating the input data, we used 50 logarithmically scale values $\sigma_0 \in [0.1, 3]$. When performing the scale selection step, we searched over a range of 80 logarithmically scale levels $\sigma \in [0.1, 5]$, and accumulated the scale-space signature over scale at the image center for each differential feature detector, and additionally performed parabolic interpolation over the logarithmic scale values to localized the scale estimates to higher accuracy. This very dense sampling of the scale levels is far beyond what is usually needed in actual computer vision algorithms, but was chosen here, in order to essentially eliminate the effects of discrete sampling issues in the scale direction.

Figure 4 shows a graph of the scale estimates obtained for the second-order Laplacian interest point detector in this way, with the corresponding relative scale errors in Figure 5. Figures 6 and 7 show corresponding results for the non-linear determinant of the second-order Hessian interest point detector.

As can be seen from these graphs, the consistency errors in the scale estimates obtained for the hybrid discretization

¹ Provided that we would not want to expand the experiments, to all possible combinations of discretization methods regarding both the input data and image operations, which would then also make the analysis and the interpretation steps more complex, this should, however, constitute an appropriate matching regarding the definition of the input data and the selection of discrete approximation method.

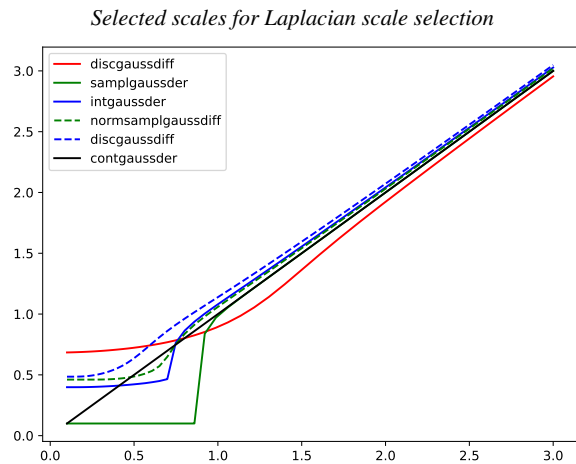


Fig. 4: Graphs of the *selected scales* $\hat{\sigma} = \sqrt{\hat{s}}$, when applying scale selection from local extrema over scale of the *scale-normalized Laplacian* response according to (21) to a set of Gaussian blobs of different size $\sigma_{\text{ref}} = \sigma_0$, for different discrete approximations of the Gaussian derivative kernels, for either discrete analogues of Gaussian derivative kernels $T_{\text{disc},x^\alpha}(n; s)$ according to (10), sampled Gaussian derivative kernels $T_{\text{sampl},x^\alpha}(n; s)$ according to (8), integrated Gaussian derivative kernels $T_{\text{int},x^\alpha}(n; s)$ according to (9), the hybrid discretization method corresponding the equivalent convolution kernels $T_{\text{hybr-sampl},x^\alpha}(n; s)$ according to (16) or the hybrid discretization method corresponding the equivalent convolution kernels $T_{\text{hybr-int},x^\alpha}(n; s)$ according to (17). For comparison, the reference scale $\sigma_{\text{ref}} = \sqrt{s_{\text{ref}}} = \sigma_0$ obtained in the continuous case for continuous Gaussian derivatives is also shown. (Horizontal axis: Reference scale $\sigma_{\text{ref}} = \sigma_0 \in [0.1, 3]$.)

Relative scale error for Laplacian scale selection

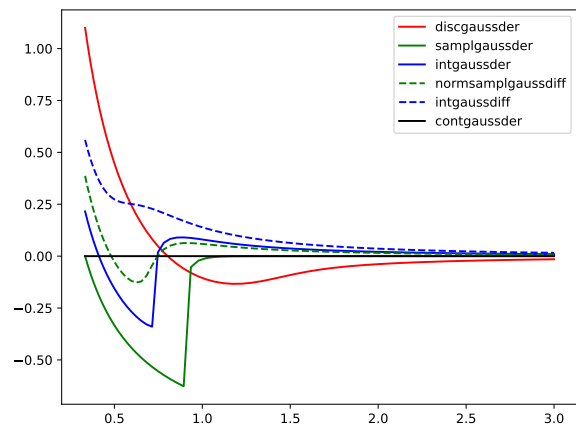


Fig. 5: Graphs of the *relative scale estimation error* $E_{\text{scaleest,rel}}(\sigma)$, according to (34), when applying scale selection from local extrema over scale of the *scale-normalized Laplacian* response according to (21) to a set of Gaussian blobs of different size $\sigma_{\text{ref}} = \sigma_0$, for different discrete approximations of the Gaussian derivative kernels, for either discrete analogues of Gaussian derivative kernels $T_{\text{disc},x^\alpha}(n; s)$ according to (10), sampled Gaussian derivative kernels $T_{\text{sampl},x^\alpha}(n; s)$ according to (8), integrated Gaussian derivative kernels $T_{\text{int},x^\alpha}(n; s)$ according to (9), the hybrid discretization method corresponding the equivalent convolution kernels $T_{\text{hybr-sampl},x^\alpha}(n; s)$ according to (16) or the hybrid discretization method corresponding the equivalent convolution kernels $T_{\text{hybr-int},x^\alpha}(n; s)$ according to (17). (Horizontal axis: Reference scale $\sigma_{\text{ref}} = \sigma_0 \in [1/3, 3]$.)

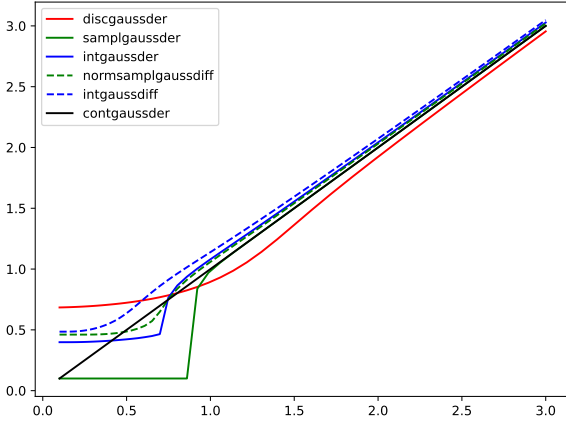
Selected scales for *detHessian* scale selection

Fig. 6: Graphs of the *selected scales* $\hat{\sigma} = \sqrt{\hat{s}}$, when applying scale selection from local extrema over scale of the *scale-normalized determinant of Hessian* response according to (22) to a set of Gaussian blobs of different size $\sigma_{\text{ref}} = \sigma_0$, for different discrete approximations of the Gaussian derivative kernels, for either discrete analogues of Gaussian derivative kernels $T_{\text{disc},x^\alpha}(n; s)$ according to (10), sampled Gaussian derivative kernels $T_{\text{sampl},x^\alpha}(n; s)$ according to (8), integrated Gaussian derivative kernels $T_{\text{int},x^\alpha}(n; s)$ according to (9), the hybrid discretization method corresponding the equivalent convolution kernels $T_{\text{hybr-sampl},x^\alpha}(n; s)$ according to (16) or the hybrid discretization method corresponding the equivalent convolution kernels $T_{\text{hybr-int},x^\alpha}(n; s)$ according to (17). For comparison, the reference scale $\sigma_{\text{ref}} = \sqrt{s_{\text{ref}}} = \sigma_0$ obtained in the continuous case for continuous Gaussian derivatives is also shown. (Horizontal axis: Reference scale $\sigma_{\text{ref}} = \sigma_0 \in [0.1, 3]$.)

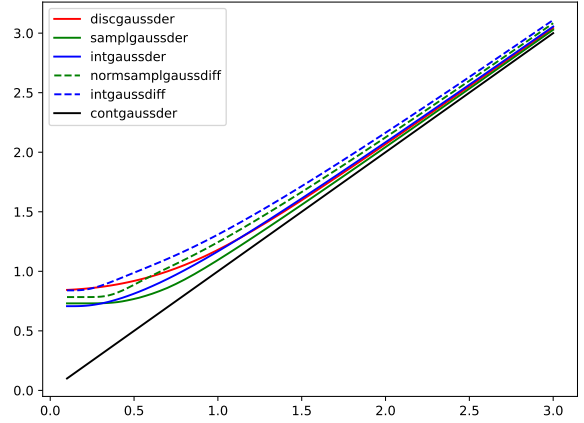
Selected scales for *gradient magnitude* scale selection

Fig. 8: Graphs of the *selected scales* $\hat{\sigma} = \sqrt{\hat{s}}$, when applying scale selection from local extrema over scale of the *scale-normalized gradient magnitude* response according to (26) to a set of diffuse step edges of different width $\sigma_{\text{ref}} = \sigma_0$, for different discrete approximations of the Gaussian derivative kernels, for either discrete analogues of Gaussian derivative kernels $T_{\text{disc},x^\alpha}(n; s)$ according to (10), sampled Gaussian derivative kernels $T_{\text{sampl},x^\alpha}(n; s)$ according to (8), integrated Gaussian derivative kernels $T_{\text{int},x^\alpha}(n; s)$ according to (9), the hybrid discretization method corresponding the equivalent convolution kernels $T_{\text{hybr-sampl},x^\alpha}(n; s)$ according to (16) or the hybrid discretization method corresponding the equivalent convolution kernels $T_{\text{hybr-int},x^\alpha}(n; s)$ according to (17). For comparison, the reference scale $\sigma_{\text{ref}} = \sqrt{s_{\text{ref}}} = \sigma_0$ obtained in the continuous case for continuous Gaussian derivatives is also shown. (Horizontal axis: Reference scale $\sigma_{\text{ref}} = \sigma_0 \in [0.1, 3]$.)

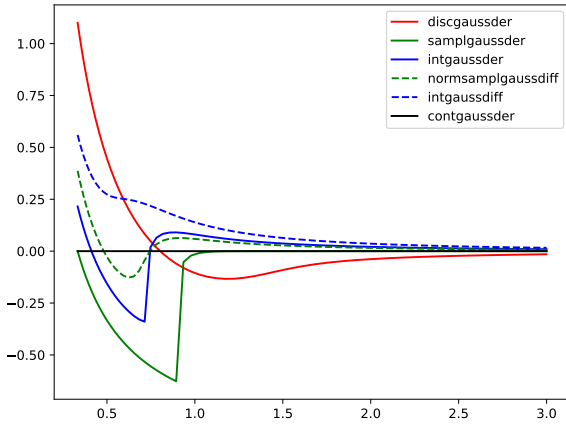
Relative scale error for *detHessian* scale selection

Fig. 7: Graphs of the *relative scale estimation error* $E_{\text{scaleest,rel}}(\sigma)$, according to (34), when applying scale selection from local extrema over scale of the *scale-normalized determinant of the Hessian* response according to (22) to a set of Gaussian blobs of different size $\sigma_{\text{ref}} = \sigma_0$, for different discrete approximations of the Gaussian derivative kernels, for either discrete analogues of Gaussian derivative kernels $T_{\text{disc},x^\alpha}(n; s)$ according to (10), sampled Gaussian derivative kernels $T_{\text{sampl},x^\alpha}(n; s)$ according to (8), integrated Gaussian derivative kernels $T_{\text{int},x^\alpha}(n; s)$ according to (9), the hybrid discretization method corresponding the equivalent convolution kernels $T_{\text{hybr-sampl},x^\alpha}(n; s)$ according to (16) or the hybrid discretization method corresponding the equivalent convolution kernels $T_{\text{hybr-int},x^\alpha}(n; s)$ according to (17). (Horizontal axis: Reference scale $\sigma_{\text{ref}} = \sigma_0 \in [1/3, 3]$.)

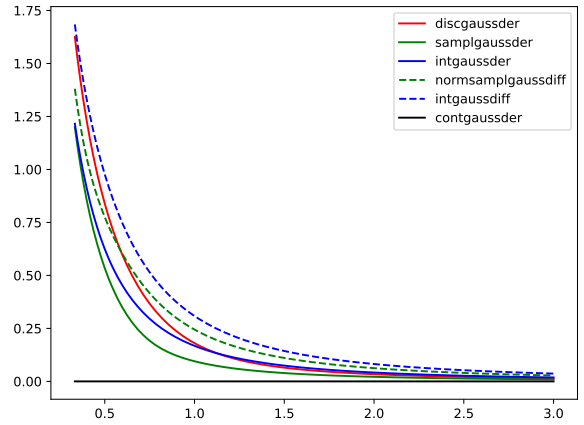
Relative scale error for *gradient magnitude* scale selection

Fig. 9: Graphs of the *relative scale estimation error* $E_{\text{scaleest,rel}}(\sigma)$, according to (34), when applying scale selection from local extrema over scale of the *scale-normalized gradient magnitude* response according to (26) to a set of diffuse step edges of different width $\sigma_{\text{ref}} = \sigma_0$, for different discrete approximations of the Gaussian derivative kernels, for either discrete analogues of Gaussian derivative kernels $T_{\text{disc},x^\alpha}(n; s)$ according to (10), sampled Gaussian derivative kernels $T_{\text{sampl},x^\alpha}(n; s)$ according to (8), integrated Gaussian derivative kernels $T_{\text{int},x^\alpha}(n; s)$ according to (9), the hybrid discretization method corresponding the equivalent convolution kernels $T_{\text{hybr-sampl},x^\alpha}(n; s)$ according to (16) or the hybrid discretization method corresponding the equivalent convolution kernels $T_{\text{hybr-int},x^\alpha}(n; s)$ according to (17). (Horizontal axis: Reference scale $\sigma_{\text{ref}} = \sigma_0 \in [1/3, 3]$.)

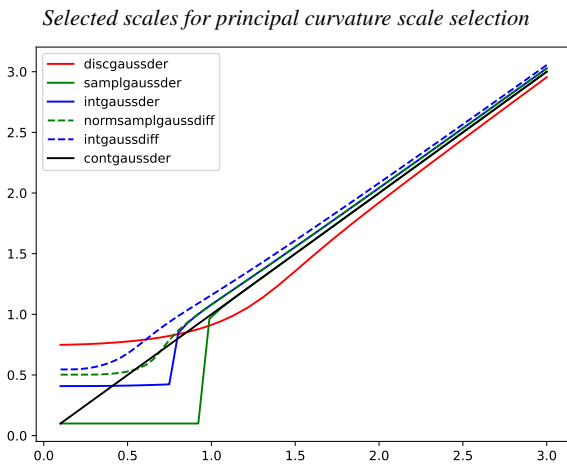


Fig. 10: Graphs of the *selected scales* $\hat{\sigma} = \sqrt{\hat{s}}$, when applying scale selection from local extrema over scale of the *scale-normalized principal curvature* response according to (30) to a set of diffuse ridges of different width $\sigma_{\text{ref}} = \sigma_0$, for different discrete approximations of the Gaussian derivative kernels, for either discrete analogues of Gaussian derivative kernels $T_{\text{disc},x^\alpha}(n; s)$ according to (10), sampled Gaussian derivative kernels $T_{\text{sampl},x^\alpha}(n; s)$ according to (8), integrated Gaussian derivative kernels $T_{\text{int},x^\alpha}(n; s)$ according to (9), the hybrid discretization method corresponding the equivalent convolution kernels $T_{\text{hybr-sampl},x^\alpha}(n; s)$ according to (16) or the hybrid discretization method corresponding the equivalent convolution kernels $T_{\text{hybr-int},x^\alpha}(n; s)$ according to (17). For comparison, the reference scale $\sigma_{\text{ref}} = \sqrt{s_{\text{ref}}} = \sigma_0$ obtained in the continuous case for continuous Gaussian derivatives is also shown. (Horizontal axis: Reference scale $\sigma_{\text{ref}} = \sigma_0 \in [0.1, 3]$.)

Relative scale error for principal curvature scale selection

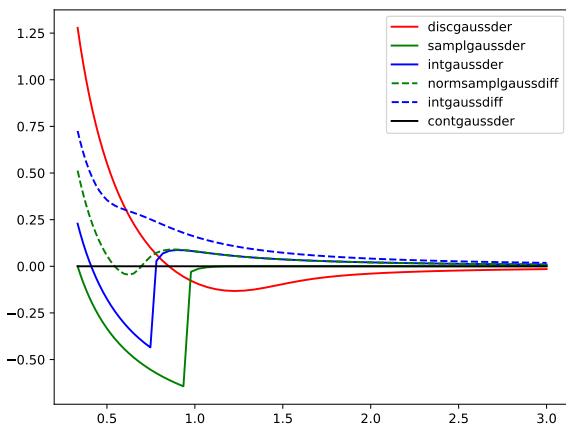


Fig. 11: Graphs of the *relative scale estimation error* $E_{\text{scaleest,rel}}(\sigma)$, according to (34), when applying scale selection from local extrema over scale of the *scale-normalized principal curvature* response according to (30) to a set of diffuse ridges of different width $\sigma_{\text{ref}} = \sigma_0$, for different discrete approximations of the Gaussian derivative kernels, for either discrete analogues of Gaussian derivative kernels $T_{\text{disc},x^\alpha}(n; s)$ according to (10), sampled Gaussian derivative kernels $T_{\text{sampl},x^\alpha}(n; s)$ according to (8), integrated Gaussian derivative kernels $T_{\text{int},x^\alpha}(n; s)$ according to (9), the hybrid discretization method corresponding the equivalent convolution kernels $T_{\text{hybr-sampl},x^\alpha}(n; s)$ according to (16) or the hybrid discretization method corresponding the equivalent convolution kernels $T_{\text{hybr-int},x^\alpha}(n; s)$ according to (17). (Horizontal axis: Reference scale $\sigma_{\text{ref}} = \sigma_0 \in [1/3, 3]$.)

methods based on either the normalized Gaussian kernel or the integrated Gaussian kernel are for larger values of the scale parameter higher than the corresponding consistency errors in the regular discretization methods based on either sampled Gaussian derivatives or integrated Gaussian derivatives. For smaller values of the scale parameter, there is, however, a range of scale values, where the consistency errors are lower for the hybrid discretization methods than for underlying corresponding regular discretization methods.

Notably, the consistency errors for the hybrid discretization methods are also generally lower for the genuinely discrete method based on convolution with the discrete analogue of the Gaussian kernel followed by central difference. In this regards, it should, however, be remarked that the scale normalization operation for the discrete analogues of Gaussian derivatives has here been performed based on a fully continuous model, while one could more generally consider deriving genuinely discrete scale normalization factors for the discretization approach based on discrete analogues of Gaussian derivatives.

Figure 8 shows the selected scale levels for the first-order gradient-magnitude-based edge detection operation, with the corresponding relative error measures shown in Figure 9. As can be seen from these graphs, the consistency errors are notably higher for the hybrid discretization approaches, compared to their underlying regular methods. In these experiments, the consistency errors are also higher for the hybrid discretization methods than for the genuinely discrete approach, based on discrete analogues of Gaussian derivatives.

Finally, Figures 10 and 11 show corresponding results for the second-order principal curvature ridge detector, which are structurally similar to the previous results for the second-order Laplacian and determinant of the Hessian interest point detectors.

5 Summary and discussion

In this paper, we have extended the in-depth treatment of different discretizations of Gaussian derivative operators in terms of explicit convolution operations in (Lindeberg 2024) to two more discretization methods, based on hybrid combinations of either convolutions with normalized sampled Gaussian kernels or convolutions with integrated Gaussian kernels with central difference operators.

The results from the treatment show that it is possible to characterize general properties of these hybrid discretization methods in terms of the effective amount of spatial smoothing that they imply, and which may for very small values of the scale parameter differ significantly from the results obtained from the fully continuous scale-space theory, as well as between different types of discretization methods.

The results from this treatment are intended to be generically applicable in situations when scale-space operations are to be applied at scale levels below the otherwise rule of thumb in classical computer vision, of not going below a certain minimum scale level, corresponding to a standard deviation of the Gaussian kernel of the order of $1/\sqrt{2}$ or 1.

One specific direct application domain for these results is when implementing deep networks in terms of Gaussian derivatives, where empirical evidence indicates that deep networks often tend to benefit from using finer scale levels than as indicated by the previous rule of thumb in classical computer vision, and which we will address in future work.

Acknowledgements

Python code, that implements a subset of the discretization methods for Gaussian smoothing and Gaussian derivatives in this paper, is available in the pycscsp package, available at GitHub:

<https://github.com/tonylindeberg/pycscsp>

as well as through PyPi:

```
pip install pycscsp
```

References

- E. J. Bekkers. B-spline CNNs on Lie groups. *International Conference on Learning Representations (ICLR 2020)*, 2020.
- H. Bouma, A. Vilanova, J. O. Bescós, B. ter Haar Romeny, and F. A. Gerritsen. Fast and accurate Gaussian derivatives based on B-splines. In *Proc. Scale Space and Variational Methods in Computer Vision (SSVM 2007)*, pages 406–417, 2007. Springer LNCS volume 4485.
- P. J. Burt and E. H. Adelson. The Laplacian pyramid as a compact image code. *IEEE Trans. Communications*, 9(4):532–540, 1983.
- D. Charalampidis. Recursive implementation of the Gaussian filter using truncated cosine functions. *IEEE Transactions on Signal Processing*, 64(14):3554–3565, 2016.
- J. L. Crowley and O. Riff. Fast computation of scale normalised Gaussian receptive fields. In L. Griffin and M. Lillholm, editors, *Proc. Scale-Space Methods in Computer Vision (Scale-Space'03)*, volume 2695 of *Springer LNCS*, pages 584–598, Isle of Skye, Scotland, 2003. Springer.
- J. L. Crowley and R. M. Stern. Fast computation of the Difference of Low Pass Transform. *IEEE Transactions on Pattern Analysis and Machine Intelligence*, 6(2):212–222, 1984.
- R. Deriche. Recursively implementing the Gaussian and its derivatives. In *Proc. International Conference on Image Processing (ICIP'92)*, pages 263–267, 1992.
- G. Farnéback and C.-F. Westin. Improving Deriche-style recursive Gaussian filters. *Journal of Mathematical Imaging and Vision*, 26(3):293–299, 2006.
- L. M. J. Florack. *Image Structure*. Series in Mathematical Imaging and Vision. Springer, 1997.
- H. Gavilima-Pilataxi and J. Ibarra-Fiallo. Multi-channel Gaussian derivative neural networks for crowd analysis. In *Proc. International Conference on Pattern Recognition Systems (ICPRS 2023)*, pages 1–7, 2023.
- J.-M. Geusebroek, A. W. M. Smeulders, and J. van de Weijer. Fast anisotropic Gauss filtering. *IEEE Transactions on Image Processing*, 12(8):938–943, 2003.
- T. Iijima. Basic theory on normalization of pattern (in case of typical one-dimensional pattern). *Bulletin of the Electrotechnical Laboratory*, 26:368–388, 1962. (in Japanese).
- J.-J. Jacobsen, J. van Gemert, Z. Lou, and A. W. M. Smeulders. Structured receptive fields in CNNs. In *Proc. Computer Vision and Pattern Recognition (CVPR 2016)*, pages 2610–2619, 2016.
- J. J. Koenderink. The structure of images. *Biological Cybernetics*, 50(5):363–370, 1984.
- J. J. Koenderink and A. J. van Doorn. Representation of local geometry in the visual system. *Biological Cybernetics*, 55(6):367–375, 1987.
- J. J. Koenderink and A. J. van Doorn. Generic neighborhood operators. *IEEE Transactions on Pattern Analysis and Machine Intelligence*, 14(6):597–605, Jun. 1992.
- J.-Y. Lim and H. S. Stiehl. A generalized discrete scale-space formulation for 2-D and 3-D signals. In *International Conference on Scale-Space Theories in Computer Vision (Scale-Space'03)*, pages 132–147, 2003. Springer LNCS volume 2695.
- T. Lindeberg. Scale-space for discrete signals. *IEEE Transactions on Pattern Analysis and Machine Intelligence*, 12(3):234–254, Mar. 1990.
- T. Lindeberg. *Scale-Space Theory in Computer Vision*. Springer, 1993a.
- T. Lindeberg. Discrete derivative approximations with scale-space properties: A basis for low-level feature extraction. *Journal of Mathematical Imaging and Vision*, 3(4):349–376, Nov. 1993b.
- T. Lindeberg. Scale-space theory: A basic tool for analysing structures at different scales. *Journal of Applied Statistics*, 21(2):225–270, 1994. Also available from <http://www.csc.kth.se/~tony/abstracts/Lin94-SI-abstract.html>.
- T. Lindeberg. Feature detection with automatic scale selection. *International Journal of Computer Vision*, 30(2):77–116, 1998a.
- T. Lindeberg. Edge detection and ridge detection with automatic scale selection. *International Journal of Computer Vision*, 30(2):117–154, 1998b.
- T. Lindeberg. Generalized Gaussian scale-space axiomatics comprising linear scale-space, affine scale-space and spatio-temporal scale-space. *Journal of Mathematical Imaging and Vision*, 40(1):36–81, 2011.
- T. Lindeberg. Scale-covariant and scale-invariant Gaussian derivative networks. In *Proc. Scale Space and Variational Methods in Computer Vision (SSVM 2021)*, volume 12679 of *Springer LNCS*, pages 3–14, 2021.
- T. Lindeberg. Scale-covariant and scale-invariant Gaussian derivative networks. *Journal of Mathematical Imaging and Vision*, 64(3):223–242, 2022.
- T. Lindeberg. Discrete approximations of Gaussian smoothing and Gaussian derivatives. *Journal of Mathematical Imaging and Vision*, 2024. preprint at arXiv:2311.11317.
- T. Lindeberg and L. Bretzner. Real-time scale selection in hybrid multi-scale representations. In L. Griffin and M. Lillholm, editors, *Proc. Scale-Space Methods in Computer Vision (Scale-Space'03)*, volume 2695 of *Springer LNCS*, pages 148–163, Isle of Skye, Scotland, 2003. Springer.
- D. G. Lowe. Distinctive image features from scale-invariant keypoints. *International Journal of Computer Vision*, 60(2):91–110, 2004.
- V. Pénau-Polge, S. Velasco-Forero, and J. Angulo. Fully trainable Gaussian derivative convolutional layer. In *International Conference on Image Processing (ICIP 2022)*, pages 2421–2425, 2022.
- S. L. Pintea, N. Tömen, S. F. Goes, M. Loog, and J. C. van Gemert. Resolution learning in deep convolutional networks using scale-space theory. *IEEE Trans. Image Processing*, 30:8342–8353, 2021.
- I. Rey-Otero and M. Delbracio. Computing an exact Gaussian scale-space. *Image Processing On Line*, 6:8–26, 2016.

- M. Sangalli, S. Blusseau, S. Velasco-Forero, and J. Angulo. Scale equivariant U-net. In *Proc. British Machine Vision Conference (BMVC 2022)*, 2022.
- E. P. Simoncelli and W. T. Freeman. The steerable pyramid: A flexible architecture for multi-scale derivative computation. In *Proc. International Conference on Image Processing (ICIP'95)*, Washington DC, 1995.
- E. P. Simoncelli, W. T. Freeman, E. H. Adelson, and D. J. Heeger. Shiftable multi-scale transforms. *IEEE Trans. Information Theory*, 38(2):587–607, 1992.
- A. Slavík and P. Stehlík. Dynamic diffusion-type equations on discrete-space domains. *Journal of Mathematical Analysis and Applications*, 427(1):525–545, 2015.
- J. Sporing, M. Nielsen, L. Florack, and P. Johansen, editors. *Gaussian Scale-Space Theory: Proc. PhD School on Scale-Space Theory*. Series in Mathematical Imaging and Vision. Springer, Copenhagen, Denmark, 1997.
- B. ter Haar Romeny. *Front-End Vision and Multi-Scale Image Analysis*. Springer, 2003.
- M. Tschirsich and A. Kuijper. Notes on discrete Gaussian scale space. *Journal of Mathematical Imaging and Vision*, 51:106–123, 2015.
- M. Unser, A. Aldroubi, and M. Eden. Fast B-spline transforms for continuous image representation and interpolation. *IEEE Transactions on Pattern Analysis and Machine Intelligence*, 13(3):277–285, 1991.
- M. Unser, A. Aldroubi, and M. Eden. B-spline signal processing. i. theory. *IEEE Transactions on Signal Processing*, 41(2):821–833, 1993.
- L. J. van Vliet, I. T. Young, and P. W. Verbeek. Recursive Gaussian derivative filters. In *International Conference on Pattern Recognition*, volume 1, pages 509–514, 1998.
- Y.-P. Wang. Image representations using multiscale differential operators. *IEEE Transactions on Image Processing*, 8(12):1757–1771, 1999.
- Y.-P. Wang and S. L. Lee. Scale-space derived from B-splines. *IEEE Transactions on Pattern Analysis and Machine Intelligence*, 20(10):1040–1055, 1998.
- J. Weickert, S. Ishikawa, and A. Imiya. Linear scale-space has first been proposed in Japan. *Journal of Mathematical Imaging and Vision*, 10(3):237–252, 1999.
- A. P. Witkin. Scale-space filtering. In *Proc. 8th Int. Joint Conf. Art. Intell.*, pages 1019–1022, Karlsruhe, Germany, Aug. 1983.
- I. T. Young and L. J. van Vliet. Recursive implementation of the Gaussian filter. *Signal Processing*, 44(2):139–151, 1995.
- Q. Zheng, M. Gong, X. You, and D. Tao. A unified B-spline framework for scale-invariant keypoint detection. *International Journal of Computer Vision*, 130(3):777–799, 2022.